Journal of Power Sources 190 (2009) 311–317

Contents lists available at ScienceDirect

Journal of Power Sources

journal homepage: www.elsevier.com/locate/jpowsour

Short communication

Silyl functionalized poly(vinylidene fluoride)/phosphotungstic acid/aminopropyltrimethoxysilane ternary composite membrane for proton conductivity

Yingbo Chen, Hern Kim*

Department of Environmental Engineering and Biotechnology, Myongji University, Yongin, Kyonggi-do 449-728, Republic of Korea

ARTICLE INFO

Article history:
Received 11 September 2008
Received in revised form 31 December 2008
Accepted 13 January 2009
Available online 30 January 2009

Keywords:
Silyl functionalized
Composite membrane
Proton conductivity
Polymer electrolyte membrane fuel cell

ABSTRACT

A novel ternary composite membrane is prepared by inverse phase separation of a mixture containing silyl functionalized poly(vinylidene fluoride) (SF-PVDF), phosphotungstic acid (PWA) and 3-aminopropyltrimethoxysilane (APTMS). The composition and structure of the resulting membranes are characterized using Fourier transform infrared spectroscopy (FTIR), thermogravimetric analysis (TGA), scanning electron microscopy (SEM) and a Universal Testing Machine (UTM). Water uptake and PWA loss of the membrane are examined for different membrane types as well as PWA amounts in the membranes. The effect of membrane type, temperature and the amounts of PWA on proton conductivity are also studied. It is found that the loss of PWA and water contained in the membrane dramatically decreases by adding suitable amounts of APTMS to the membranes. The novel ternary composite membrane, with good mechanical strength and thermal stability, can reach a proton conductivity of 0.01 S cm^{-1} under moderate conditions.

1. Introduction

A proton conductive membrane is a key component for advanced polymer electrolyte membrane fuel cells. Good permeability, conductivity and mechanical stability are essential for usage of the membranes at moderate temperature. A number of preparation methods have been developed to enhance the performance of fuel cell membranes such as sulfonation [1,2], polymer blends [3–6], crosslinking [7–9], addition of fillers [10–13] and the sol–gel method [14–17]. These methods, however, can hardly satisfy the required properties for polymer electrolyte membranes. For example, sulfonation of a polymer can considerably increase proton conductivity at the expense of losing mechanical stability and increasing fuel permeability. Particularly, when the operating temperature is higher than 100 °C, the proton conductivity of a sulfonated polymeric electrolyte membrane, such as Nafion, drops dramatically because of dehydration. Therefore, it has been a challenging issue to develop a novel membrane material with high proton conductivity, low fuel permeation, and good mechanical and thermal properties for fuel cell applications.

Poly(vinylidene fluoride) (PVDF) is an excellent material for membranes due to its advantages of easy membrane formation, high strength, and good resistance to solvents, acids and bases. Because of this, a number of materials based on PVDF are widely employed as a component of fuel cell membranes. PVDF blends such as polyetheretherketone–poly(vinylidene fluoride) (PEEK–PVDF) [18] and nafion–PVDF [19] have been successfully used for direct methanol fuel cells to decrease methanol permeability. In addition, PVDF graft copolymers [20] with sulfonated polymer side-chains have been used as electrolytes with good thermal stability up to 350 °C. Furthermore, PVDF composite membranes such as PVDF–HFP–PEG–Al_2O_3 [21] and PVDF–heteropoly acid (HPA) [22] have also used as solid-state membranes for fuel cells. Nevertheless, the poor compatibility of PVDF with other inorganic materials, such as HPA, limits its application in composite materials. Thus, one of the objectives of this study is to modify PVDF with silyl groups by grafting 3-(trimethoxysilyl) propyl methacrylate (TMSPMA) via atom transfer radical polymerization (ATRP), making the modified PVDF compatible with heteropolyacid in polar solvents.

Heteropoly acids, such as phosphotungstic acid (PWA) [23], have long been characterized as solid acids with high proton conductivity due to their dense, hydrogen-bonded hydration water network. This water network is stable even at the temperatures higher than 100 °C. A problem arose, however, when HPAs were directly mixed with the substrate materials [13]; they tend to flow out of the composites after being used for a short period of time. In this study, such problem is prevented by incorporating PWA with a silica network which is grafted to PVDF macromolecular chains. Since PWA [24] has strong interaction with amino groups, addition of 3-

* Corresponding author. Tel.: +82 31 330 6688; fax: +82 31 336 6336.
E-mail address: hernkim@mju.ac.kr (H. Kim).

0378-7753/$ – see front matter © 2009 Elsevier B.V. All rights reserved.
doi:10.1016/j.jpowsour.2009.01.053

aminopropyltrimethoxysilane (APTMS) to the silica network in the membrane can decrease the leaking of PWA.

In order to get a highly conductive membrane with excellent mechanical strength and thermal stability, silyl functionalized PVDF, PWA and APTMS are used to prepare the ternary composite membrane. The grafted PVDF with PTMSPMA side-chains offers reaction sites for APTMS. The hydrolysis of PTMSPMA side-chains and APTMS produces the silica networks or particles in which the amino groups can react with PWA to form ionic bonds. This kind of bonding is helpful for keeping the PWA in the composite membrane and thus increasing the conductivity. The formation of silica network contributes to the mechanical property of the composite membranes.

2. Experimental

2.1. Materials

PVDF (Solvey 6013/1001 M_w ca. 2.2×10^5 g mol^{-1}) was received from Solvey Korea Co. Phosphotungstic acid, 1-methyl-2-pyrrolidinone (NMP), copper (I) chloride (CuCl), 4,4′-dimethyl-2,2′-dipyridyl (DMDP), 3-(trimethoxysilyl) propyl methacrylate, 3-aminopropyltrimethoxysilane, ether, and ammonia water (28 wt.%) were purchased from Aldrich Chemical Co.

2.2. Synthesis of grafted PVDF

PVDF-g-PTMSPMA grafted polymers [25] were synthesized by ATRP using PVDF as the macro-initiator. From the secondary fluorine atoms of PVDF, TMSPMA was initiated by CuCl and DMDP in an NMP solution. A typical procedure is given as follows. Five grams of PVDF were dissolved in 45 ml NMP in a round-bottom flask and mixed using a magnetic stirrer at 60 °C. After complete dissolution of the PVDF, the solution was cooled to room temperature. Then, CuCl (0.083 g), DMDP (0.155 g) and TMSPMA (10 ml) were added, and the flask was sealed with a rubber septum. In order to remove the dissolved oxygen, argon gas was bubbled through a needle that penetrated through the rubber septum and into the mixed solution for 30 min with constant stirring. The flask was then transferred to an oil bath which was preheated at 90 °C. The reaction was allowed to proceed for 20 h and the reaction mixture was precipitated in ether. For further purification, the grafted polymer was redissolved in NMP and re-precipitated three times in ether. The precipitated grafted polymer was filtered with a Buchner funnel and dried under vacuum at room temperature for 48 h.

2.3. Membrane preparation

The composite membranes containing silyl functionalized PVDF (SF-PVDF) and PWA were prepared using a solvent evaporation method. As a comparison, pure PVDF and a crosslinker 3-aminopropyltrimethoxysilane were also used to prepare the membranes. The components and the corresponding codes of the different membranes are listed in Table 1. As a component of the membrane, PWA also serves as a catalyst for the hydrolysis of silyl groups in the functional PVDF or APTMS. In detail, (silyl functionalized) PVDF, PWA and APTMS (if used) were dissolved in NMP and stirred until a homogeneous solution was obtained. The solution was poured in a Teflon Petri dish and dried in a vacuum oven at room temperature for solvent evaporation. After the membrane was formed, the temperature was increased to 80 °C to remove the excess solvent.

2.4. Membrane characterization

2.4.1. Water uptake and PWA loss determination

Water uptake and PWA loss were measured by the weight difference between the dried and wet membranes. A piece of the membrane was dried in vacuum at 150 °C to obtain a constant weight (W_0), and was then immersed in water for 24 h. The wet membrane was then weighed (W_1) after removing the surface water using tissue paper. Finally, the membrane was again dried in vacuum at 150 °C and weighed (W_2). The weight of each membrane was then measured for at least three times to obtain an approximately constant weight. The PWA loss is calculated by:

$$\text{PWA loss (wt.\%)} = \frac{W_0 - W_2}{W_0} \quad (1)$$

Water uptake is recorded by:

$$\text{water uptake (wt.\%)} = \frac{W_1 + (W_0 - W_2) - W_0}{W_1 + (W_0 - W_2)} \quad (2)$$

2.4.2. Proton conductivity determination

The proton conductivity of the membranes was measured using a.c. impedance spectroscopy (IM6EX, Zahn) over a frequency range of 20 mHz–1 MHz in galvanostatic mode, with an a.c. current amplitude of 10 μA using a four-point-probe method. The membrane was cut into 1×4 cm and clamped between the electrodes. The measurement was taken in a sealed flask with a little amount of water at temperatures ranging from 20 to 100 °C. The resistance value was read from the Nyquist graph of the spectroscopy. Proton conductivity was calculated by:

$$\rho = \frac{L}{R \times d \times D} \quad (3)$$

where: ρ is the proton conductivity; L (1 cm) is the distance between the sensing electrodes; d is the thickness of the membrane, which was measured using a micrometer; D (1 cm) is the width of the membrane.

2.4.3. Characterization

Fourier transform infrared spectroscopy (FTIR, Varian 2000) was used to obtain the spectra of the membranes. All spectra were acquired by signal averaging 32 scans at a resolution of 8 cm^{-1} in attenuated total reflection (ATR) mode. Thermal degradation of the

Table 1
Loss of PWA and water uptake of membranes.

Membrane composites	Polymer (mg)	PWA (mg)	APTMS (mg)	PWA loss (wt.%)	Water uptake (wt.%)
SF-PVDF/PWA-1	200	50	–	0.23	1.14
SF-PVDF/PWA-2	200	100	–	2.18	1.79
SF-PVDF/PWA-3	200	200	–	16.4	1.03
SF-PVDF/PWA-4	200	400	–	50.3	6.39
PVDF/PWA	200	200	–	13.7	3.39
SF-PVDF/PWA/NH_2SiO_2-1	200	200	50	1.42	3.25
SF-PVDF/PWA/NH_2SiO_2-2	200	200	20	3.11	6.77
PVDF/PWA/NH_2SiO_2-1	200	200	50	6.32	3.06
PVDF/PWA/NH_2SiO_2-2	200	200	20	2.57	2.70
PVDF/PWA/NH_2SiO_2-3	200	400	20	37.5	6.57

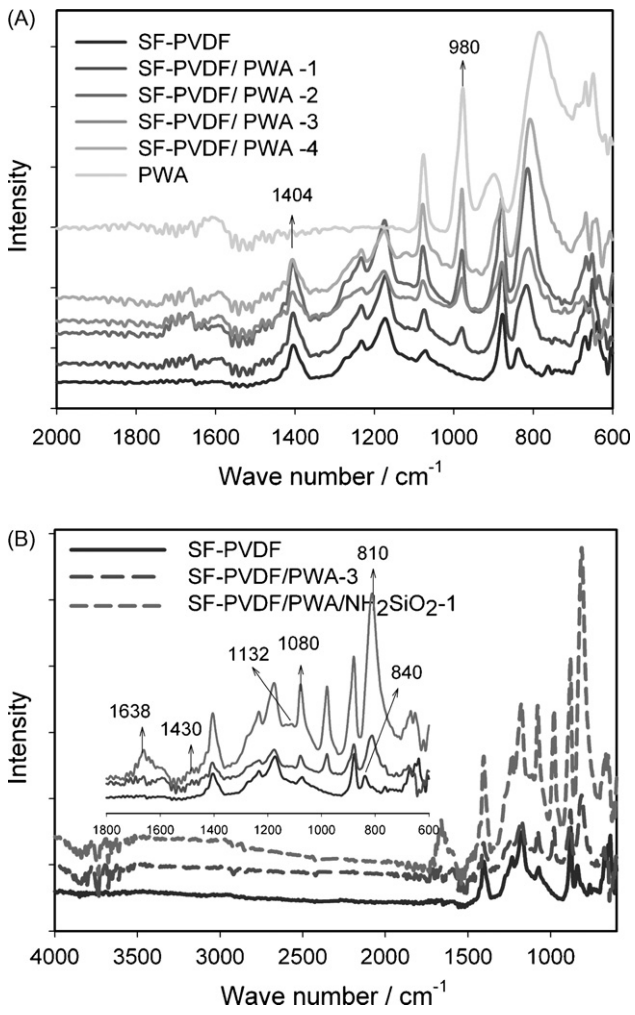

Fig. 1. FTIR spectra of membranes.

membranes was also measured using thermogravimetric analysis (TGA, TG/DSC 92, Setaram) by heating the samples from 60 to 800 °C at a heating rate of 10 °C min^{-1} under a nitrogen atmosphere. All mechanical testing was performed by means of a Universal Testing Machine (UTM LF Plus, Lloyd), equipped with a 1 kN load cell. The test was conducted at a cross-head speed of 10 mm min^{-1}. Scanning electron microscopy (SEM) images were obtained with a Hitachi S-3500N SEM. The specimens were sputtered with gold in a high-vacuum evaporator before examination.

3. Results and discussion

3.1. FTIR spectra of membranes

As demonstrated in Fig. 1(A), the absorption peak that appears at 980 cm^{-1} is attributed to the vibration of the W–O band [26] in PWA. Whereas, the characteristic vibration of the C–F band in silyl functionalized PVDF appears at 1404 cm^{-1}. The relative intensity of these two peaks shows the corresponding contents of the two components, PWA and silyl functionalized PVDF, in the composites. The ratio of the intensity of the two peaks (I_{980}/I_{1404}) increases from 0.37 to 1.20, 1.69, and 2.78 when increasing the content of PWA from 20 to 33, 50, and 67 wt.%, respectively.

Moreover, the ATR absorption peaks of silyl functionalized PVDF and its binary and ternary composite membranes are indicated in Fig. 1(B). The peaks at 3200–3700 cm^{-1} are attributed to the hydroxyl groups of water contained in PWA. The increase in the intensity of the band of siloxane (–Si–O–Si–) at 1080 cm^{-1} and the shifting of the peaks of Si–OR (from 840 to 810 cm^{-1}) are due to the hydrolysis of siloxanes (PTMSPMA side-chains and APTMS). Furthermore, the peaks of amino groups are shown at 1430 cm^{-1} for NH_2 stretching, 1638 cm^{-1} for N–H bending vibration [27] and 1132 cm^{-1} for N–H deformation. The peaks appearing around 1600 cm^{-1} can be attributed to the deformational vibrations [28] of adsorbed water molecules.

3.2. PWA loss and water uptake

The proton conductivity of polymeric electrolyte membranes depends on the components and structures of the membranes at the same temperature and humidity. PWA, combined with a large amount of water molecules around its Keggin structure, makes it suitable for proton conductivity. In this study, the proton conductivity of PVDF–PWA membranes varies with the amount of PWA included in the membrane. This is because PWA serves as the proton-transfer site and its interaction with water molecules forms the channel for proton transportation in the membrane. It is evident that the amount of transfer sites increases as the amount of PWA increases, although partial PWA is lost as seen in Table 1. Hence the water uptake of the membranes increases with the amount of PWA in the membrane. As observed, PWA loss is 50 wt.% when the amount of PWA in the membrane is 67 wt.%. The loss of PWA definitely influences the proton conductivity of the membranes. Therefore, a strategy was used to decrease the PWA loss by adding APTMS to form a ternary composite. The addition of APTMS fulfils two roles: (1) to form crosslinking of SF-PVDF or PVDF polymer in the membranes by hydrolysis of methoxysilanes; (2) to enhance the interaction with PWA by supplying amine groups. PWA itself acts as a catalyst and provides water for the hydrolysis of APTMS and PTMSPMA side-chains in SF-PVDF. The PWA loss decreases dramatically by adding APTMS both in PVDF and SF-PVDF membranes, as shown in Table 1. By adding 50 mg APTMS in the membrane, water uptake increases three times in SF-PVDF composite membranes, whereas it decreases a little in PVDF composite membranes. The different water uptake in the two types of composite membrane is due to the formation of different microstructures in the membrane (see Fig. 2). In the PVDF composite membrane, APTMS tends to aggregate to form particles dispersing in the PVDF phase. PWA either attaches to the formed particles or is dispersed in the PVDF polymer phase. However, the existence of silyl side groups in the silyl functionalized PVDF allows APTMS to combine with SF-PVDF and form a network structure with amine groups appending freely. These free amine groups have strong interaction with PWA.

3.3. Mechanical and thermal properties

The structural differences of the membranes can also be confirmed from the differences in their ability to handle mechanical stress. In Fig. 3, the silyl functionalized PVDF membrane shows a lower stress compared with the pure PVDF membrane. After blending with PWA, both membranes decrease their stress by around half. By increasing the amount of PWA, the stress of SF-PVDF/PWA binary membranes also decreases. Addition of APTMS slightly decreases the stress for both types of membranes. On the other hand, the extension-to-break of the ternary membrane is much higher than that of the binary membrane. Moreover, the effect of the different amounts of APTMS on the mechanical properties of the two types of membrane is different. In SF-PVDF/PWA/NH_2SiO_2 ternary membranes, more APTMS results in higher stress as well as higher extension. In other words, more APTMS in the membrane will help increase its toughness. The formation of a network structure should be responsible for this increase in toughness. On the con-

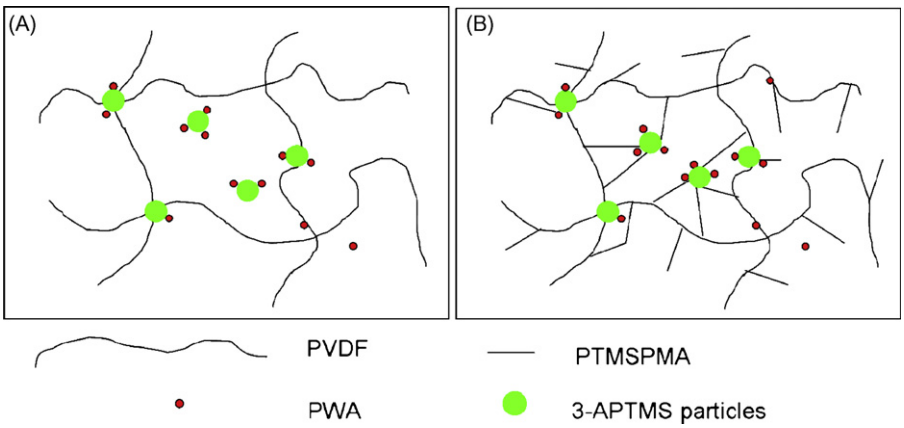

Fig. 2. Scheme of structures of ternary composite membranes (A) PVDF/PWA/APTMS and (B) SF-PVDF/PWA/APTMS.

trary, more APTMS leads to lower stress and lower extension (or lower toughness) in PVDF/PWA/NH_2SiO_2 ternary membranes. At lower amounts of APTMS, it acts as a plasticizer which enhances the toughness of the membrane. As more APTMS is added, however, it tends to form particles under the catalysis of PWA and thus decreases the toughness of the membrane.

Thermal gravimetric analysis, as shown in Fig. 4, reveals that the degradation temperature of the composite membranes is lower than those of their corresponding pure membranes. This decrease in degradation temperature can be attributed to the influence of the addition of PWA on the crystallinity of PVDF or SF-PVDF. This influence is much stronger in the PVDF composite membrane than in the SF-PVDF composite membrane since the degradation temperature of the PVDF composite membrane decreases from 440 to 370 °C, whereas for the SF-PVDF composite membrane, it decreases from 420 to 400 °C.

3.4. SEM images of membranes

The surface morphologies of the membranes prepared from PVDF/PWA and SF-PVDF/PWA with or without APTMS were observed using SEM. Fig. 5(A) and (B) shows the surface images of PVDF/PWA and SF-PVDF/PWA membranes, each with 50 wt.% of PWA. In the PVDF/PWA composite membrane, aggregation of PWA on the surface can be identified in Fig. 5(A). By contrast, a uniform surface forms in the SF-PVDF/PWA composite membrane. Self-hydrolysis of PTMSPMA side-chains catalyzed by PWA makes SF-PVDF more compatible with PWA and results in a regular surface structure.

A more interesting phenomenon appears when APTMS is added in the membranes, as shown in Fig. 5(C) and (D). A dense surface layer is formed with evenly distributed micropores, with a size of around 4.5 and 8.2 μm, measured from Fig. 5(G) and (H) in PVDF/PWA/APTMS and SF-PVDF/PWA/APTMS ternary membranes, respectively. The formation of the dense surface layer can be explained through the hydrolysis of APTMS, wherein it tends to move to the surface of the membranes. The pores on the surface layer in the SF-PVDF/PWA/APTMS membrane are larger than those

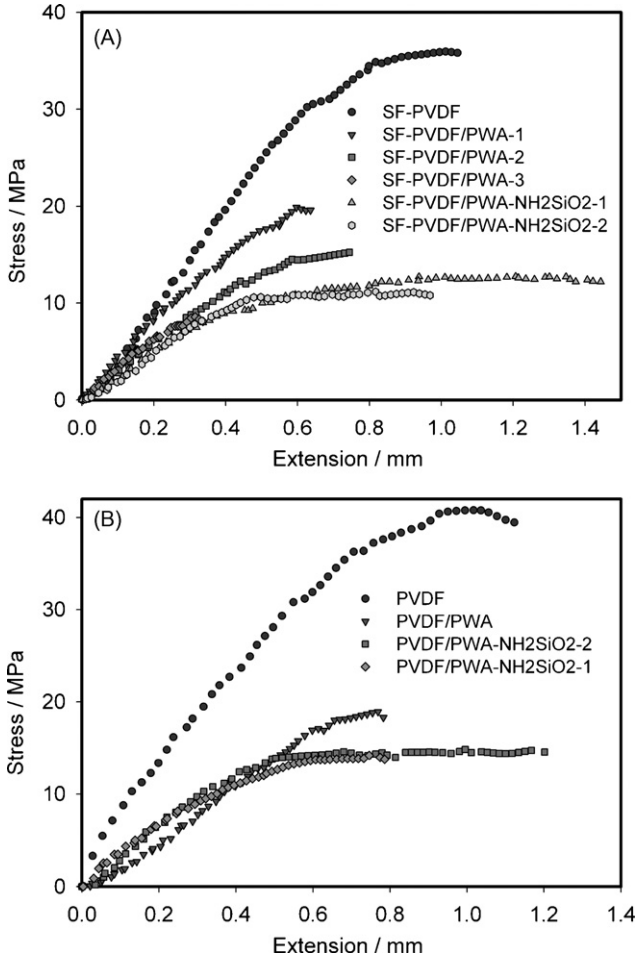

Fig. 3. Mechanical properties of membranes.

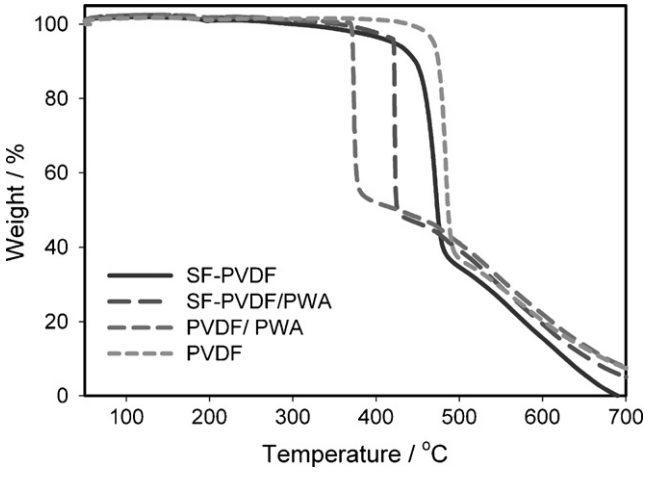

Fig. 4. TGA curves of membranes.

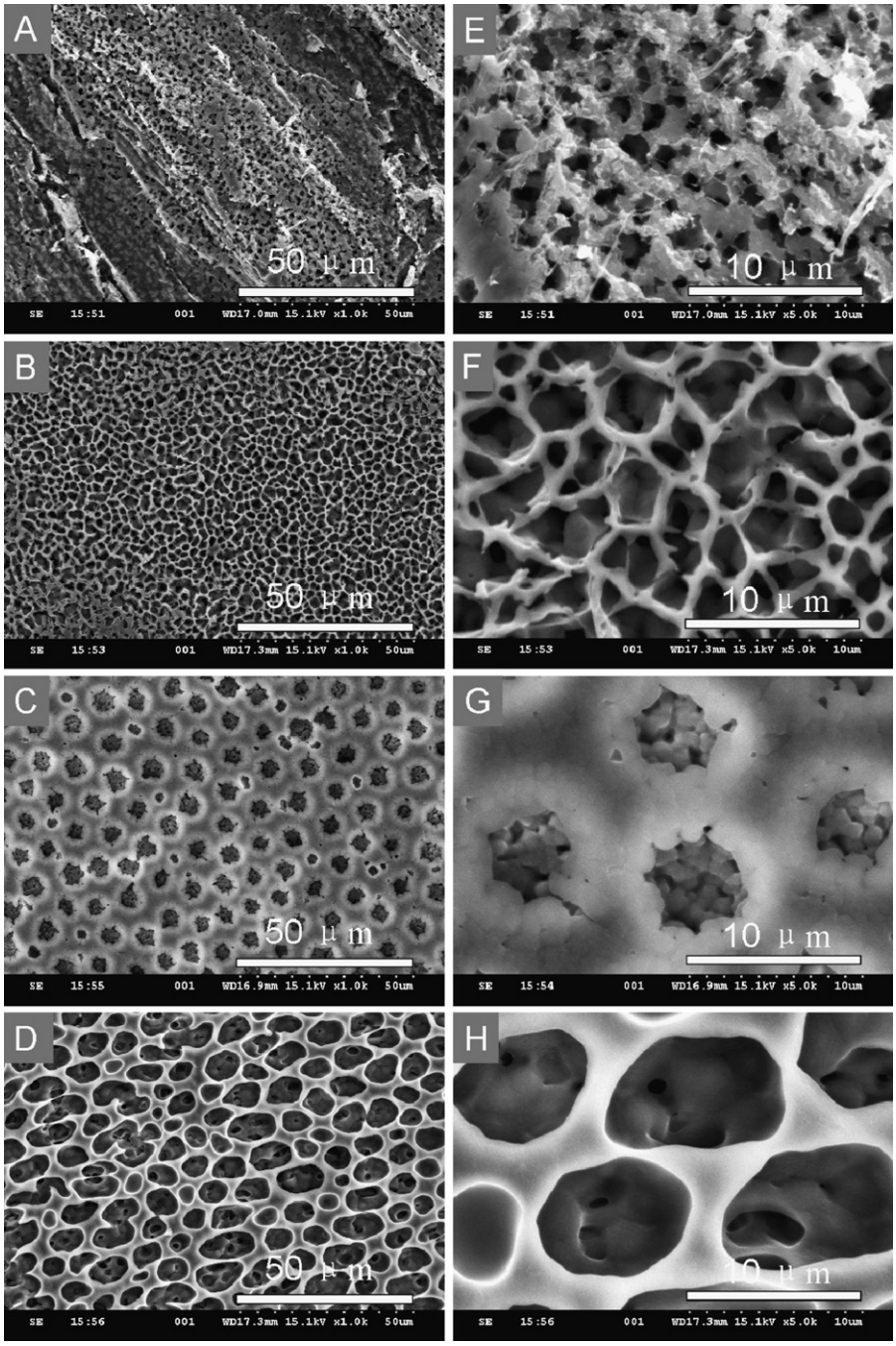

Fig. 5. SEM images of (A) PVDF/PWA, (B) SF-PVDF/PWA, (C) PVDF/PWA/APTMS, and (D) SF-PVDF/PWA/APTMS. (E), (F), (G), and (H) are images with higher magnification, correspondingly.

in the PVDF/PWA/APTMS membrane because of less hydrolyzed APTMS, which is bonded with TMSPMA side-chains, can move to the surface. The dense layer with micropores containing hydrophilic NH_2 groups decreases the PWA loss and increases the water uptake, thus increasing the proton conductivity.

3.5. Proton conductivity of membranes

The proton conductivities of the four different types of membrane with 50 wt.% PWA and 50 mg APTMS for the ternary membranes were measured using a four-point-probe method. As shown in Fig. 6, although the addition of APTMS to the membranes considerably decreases the loss of PWA, their proton conductivities remain lower compared with their corresponding binary membranes; and even at higher temperatures, the difference in their proton conductivities decreases. The formation of a network by the hydrolysis of APTMS, which hinders the transportation of protons, is responsible for this low proton conductivity. Therefore, fewer amounts of APTMS should be used to find a balance between PWA loss and proton conductivity. The effects of the amount of APTMS will be discussed later on. Herein, the focus is placed on the effect of temperature on the proton conductivities of the four types of membrane. The proton conductivity of the binary membranes follows the same rule, that is, increasing at first to a maximum at 60 °C and then decreasing as the temperature is further increased. The increasing proton conductivity at temperatures lower than 60 °C can be

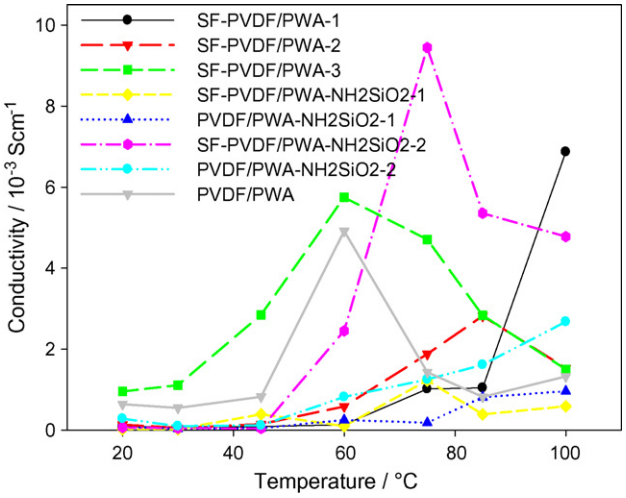

Fig. 6. Proton conductivity of different membranes with temperatures.

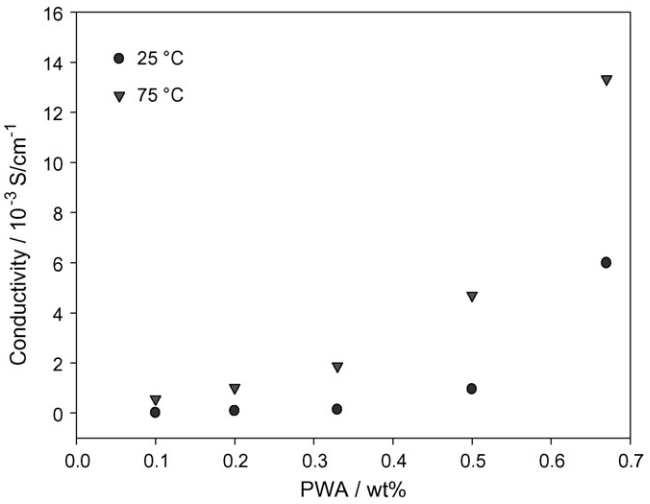

Fig. 7. Proton conductivity of membranes with different amounts of PWA.

attributed to the augmented diffusion of the proton in the polymer composite membranes. At a temperature higher than 60 °C, proton conductivity decreases with increasing temperature, which is due to a loss of both PWA and water. Proton conductivity depends on three factors: (1) the mobility of protons in the membranes; (2) the amount of PWA left in the membranes; (3) the amount of water in the membranes. Thus, the conductivity of the ternary membranes varies with temperature irregularly. The individual effect of each factor in the binary membranes is investigated in the next section.

3.6. Effect of temperature and amount of PWA on proton conductivity

The proton conductivity of the binary membranes was measured at different temperatures from 20 to 100 °C at water vapour by holding the membrane over a water reservoir. Each measurement was carried at a fixed temperature after the set temperature has been reached for 15 min. Generally, the proton conductivities of the membranes increase with increasing amounts of PWA added in the membranes at temperatures from 20 to 100 °C. Only the proton conductivities of membranes with 20 wt.% PWA directly increase with temperature. Especially after 45 °C, the proton conductivity sharply increases and is even higher than that of the membrane containing 67 wt.% of PWA measured at 100 °C. When the amount of PWA is higher than 33 wt.%, however, the proton conductivities of the membranes tend to reach a maximum and then decrease with temperature. In addition, membranes with greater amounts of PWA reach their maximum conductivities at lower temperatures (see Fig. 6).

The proton conductivities of the membranes increase with increasing amount of PWA, both at room temperature (25 °C) and at a higher temperature (75 °C) as seen from Fig. 7. The rate of increase at room temperature, however, is much faster than that at 75 °C. Moreover, the difference in the conductivity between those measured at room temperature and at high temperature becomes smaller with an increasing amount of PWA added in the membranes.

3.7. Effect of APTMS on proton conductivity

APTMS plays a very important role in the proton conductivity of the membrane (see Fig. 6). First, it forms a network with the polymers to stop PWA from leaking out of the membrane. Second, its amine groups interact and attach with PWA to form channels for proton transportation. It can be seen that the ternary membranes with 50 mg APTMS have lower conductivity than the corresponding binary membrane. The reason for this decrease in proton conductivity is the formation of tight silica networks and this hinders the transportation of protons in the membrane. Therefore, fewer amounts of APTMS (20 mg) were added in the membranes to observe the changes in conductivity. Both ternary membranes prepared from PVDF and SF-PVDF show an increase in proton conductivity of 1–2 magnitude. SF-PVDF ternary membranes have higher conductivities than their corresponding PVDF ternary membranes. In addition, a conductivity of 0.01 S cm^{-1} can be reached at 70 °C with the SF-PVDF/PWA/APTMS ternary composite membrane.

4. Conclusions

A ternary composite membrane SF-PVDF/PWA/APTMS has been prepared using APTMS as an anchor for keeping PWA in the membrane structure by the hydrolysis of the silane groups in the side-chains of SF-PVDF and in APTMS. PWA acts as a catalyst for both the hydrolysis of silane groups as well as for proton conductivity. The prepared ternary composite membranes have good mechanical and thermal properties due to the formation of network structures. The addition of APTMS dramatically decreases the leakage of PWA and thus enhances the proton conductivity of the membranes. The amount of APTMS has an obvious influence on the conductivity of the ternary membranes and a proton conductivity of 0.01 S cm^{-1} can be reached at 70 °C with 20 mg APTMS added in the membrane.

Acknowledgement

This work was financially supported by BK21 program, Republic of Korea.

References

[1] H. Zhang, J. Pang, D. Wang, A. Li, X. Li, Z. Jiang, J. Membr. Sci. 264 (2005) 56–64.
[2] Z. Shi, S. Holdcroft, Macromolecules 38 (2005) 4193–4201.
[3] R.Q. Fu, D. Julius, L. Hong, J.Y. Lee, J. Membr. Sci. 322 (2008) 331–338.
[4] J.V. Gasa, R.A. Weiss, M.T. Shaw, J. Membr. Sci. 320 (2008) 215–223.
[5] S. Pasupathi, S. Ji, B. Jan Bladergroen, V. Linkov, Int. J. Hydrogen Energy 33 (2008) 3132–3136.
[6] N.Y. Arnett, W.L. Harrison, A.S. Badami, A. Roy, O. Lane, F. Cromer, L. Dong, J.E. McGrath, J. Power Sources 172 (2007) 20–29.
[7] L. Wu, T. Xu, J. Membr. Sci. 322 (2008) 286–292.
[8] Y. Xiong, Q.L. Liu, Q.G. Zhang, A.M. Zhu, J. Power Sources 183 (2008) 447–453.
[9] A. Anis, A.K. Banthia, S. Bandyopadhyay, J. Power Sources 179 (2008) 69–80.
[10] P. Mustarelli, A. Carollo, S. Grandi, E. Quartarone, C. Tomasi, S. Leonardi, A. Magistris, Fuel Cells 7 (2007) 441–446.

[11] P. Gómez-Romero, J.A. Asensio, S. Borrós, Electrochim. Acta 50 (2005) 4715–4720.
[12] P. Staiti, M. Minutoli, J. Power Sources 94 (2001) 9–13.
[13] M.L. Ponce, L. Prado, B. Ruffmann, K. Richau, R. Mohr, S.P. Nunes, J. Membr. Sci. 217 (2003) 5–15.
[14] H. Sato, T. Norisuye, T. Takemori, Q. Tran-Cong-Miyata, S. Nomura, Polymer 48 (2007) 5681–5687.
[15] M. Aparicio, J. Mosa, M. Etienne, A. Durán, J. Power Sources 145 (2005) 231–236.
[16] D.R. Vernon, F. Meng, S.F. Dec, D.L. Williamson, J.A. Turner, A.M. Herring, J. Power Sources 139 (2005) 141–151.
[17] U. Lavrenčič Štangar, B. Orel, J. Vince, V. Jovanovski, H. Spreizer, A. Šurca Vuk, S. Hočevar, J. Solid State Electrochem. 9 (2005) 106–113.
[18] J. Wootthikanokkhan, N. Seeponkai, J. Appl. Polym. Sci. 102 (2006) 5941–5947.
[19] S.W. Choi, Y.Z. Fu, Y.R. Ahn, S.M. Jo, A. Manthiram, J. Power Sources 180 (2008) 167–171.
[20] Y.W. Kim, D.K. Lee, K.J. Lee, J.H. Kim, Eur. Polym. J. 44 (2008) 932–939.
[21] G.G. Kumar, P. Kim, K. Nahm, R.N. Elizabeth, J. Membr. Sci. 303 (2007) 126–131.
[22] J.L. Malers, M.A. Sweikart, J.L. Horan, J.A. Turner, A.M. Herring, J. Power Sources 172 (2007) 83–88.
[23] O. Nakamura, I. Ogino, T. Kodama, Solid State Ionics 3–4 (1981) 347–351.
[24] M.L. Ponce, L.A.S. de, A. Prado, V. Silva, S.P. Nunes, Desalination 162 (2004) 383–391.
[25] Y. Chen, H. Kim, React. Funct. Polym. 68 (2008) 1499–1506.
[26] T. Inoue, T. Uma, M. Nogami, J. Membr. Sci. 323 (2008) 148–152.
[27] J.H. Chen, Q.L. Liu, X.H. Zhang, Q.G. Zhang, J. Membr. Sci. 292 (2007) 125–132.
[28] S. Srisuda, B. Virote, J. Environ. Sci. 20 (2008) 379–384.